

BinaryAttention: One-Bit QK-Attention for Vision and Diffusion Transformers

Chaodong Xiao^{1,2}, Zhengqiang Zhang^{1,2}, Lei Zhang^{1,2,†}
¹The Hong Kong Polytechnic University ²OPPO Research Institute
 chaodong.xiao@connect.polyu.hk, cslzhang@comp.polyu.edu.hk

Abstract

Transformers have achieved widespread and remarkable success, while the computational complexity of their attention modules remains a major bottleneck for vision tasks. Existing methods mainly employ 8-bit or 4-bit quantization to balance efficiency and accuracy. In this paper, with theoretical justification, we indicate that binarization of attention preserves the essential similarity relationships, and propose **BinaryAttention**, an effective method for fast and accurate 1-bit qk-attention. Specifically, we retain only the sign of queries and keys in computing the attention, and replace the floating dot products with bit-wise operations, significantly reducing the computational cost. We mitigate the inherent information loss under 1-bit quantization by incorporating a learnable bias, and enable end-to-end acceleration. To maintain the accuracy of attention, we adopt quantization-aware training and self-distillation techniques, mitigating quantization errors while ensuring sign-aligned similarity. BinaryAttention is more than $2\times$ faster than FlashAttention2 on A100 GPUs. Extensive experiments on vision transformer and diffusion transformer benchmarks demonstrate that BinaryAttention matches or even exceeds full-precision attention, validating its effectiveness. Our work provides a highly efficient and effective alternative to full-precision attention, pushing the frontier of low-bit vision and diffusion transformers. The codes and models can be found at <https://github.com/EdwardChasel/BinaryAttention>.

1. Introduction

Transformers [74] have made great breakthroughs in different fields, from natural language processing [6, 11, 17, 26, 60, 71, 73], to vision tasks [10, 18, 30, 49, 56, 62, 68], and to multimodal fundamental models [1, 41, 42, 48, 59, 75], largely due to the expressivity of attention mechanism. Despite the remarkable progress, this success comes with a cost: standard attention scales quadratically with sequence length, creating extraordinary computational resources demand for

[†]Corresponding author. This research is supported by the PolyU-OPPO Joint Innovative Research Center.

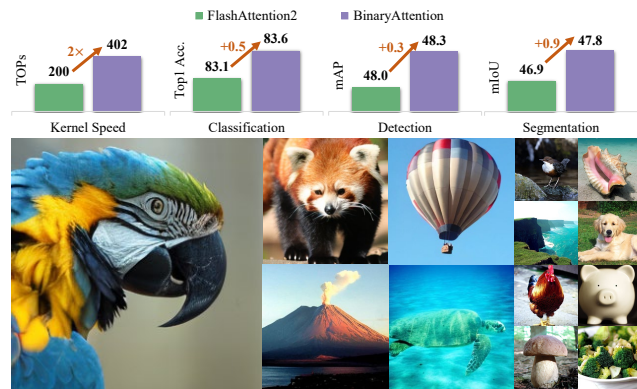


Figure 1. **Top:** Performance comparison between FlashAttention2 and BinaryAttention on vision tasks. **Bottom:** Image generation examples by DiT-XL/2 [56] driven by BinaryAttention.

long-context and high-resolution tasks. To alleviate this bottleneck, significant efforts [15, 22, 23, 58, 67, 70] have been dedicated to accelerating Transformers. These approaches can be broadly grouped into the *architecture optimization*, *model quantization*, and *hardware optimization* categories.

Architecture optimization seeks to reduce computational overhead by revising the attention mechanism. Linear attention [2, 37, 76, 82, 84] replaces quadratic dot-product operations with linear complexity kernel computations. Sparse attention [3, 21, 63, 69, 78, 85] restricts computations to a selected subset of token pairs. More recent state space models [14, 23, 25] substitute the standard attention with a recurrent data-dependent selection mechanism. While effective, these methods often struggle to maintain the expressive power of standard attention across diverse models and tasks.

Model quantization [9, 22, 36] is a principled approach to accelerate training and inference while shrinking memory by reducing numerical precision. The quantization of linear layers has been explored in depth [20, 31, 39, 44, 46, 50, 51, 79, 81] and is relatively mature. In contrast, recent efforts such as SageAttention [87–89] have increasingly focused on the quantization of attention. Unlike linear layers, quantizing attention presents unique challenges due to the dynamic nature and the sensitive softmax normalization. Consequently, these approaches typically employ 8-bit or 4-bit representa-

tions (*e.g.*, INT8, FP8, INT4 and FP4) to maintain a practical balance between efficiency and accuracy. However, further reduction of the precision to sub-4-bit levels, especially to binary representations, remains a major hurdle, as the extreme information loss and optimization instability cause an abrupt performance degradation.

Hardware optimization leverages specialized hardware designs and kernel optimizations to accelerate Transformers. Breakthroughs such as FlashAttention [13, 15, 65] achieve significant speedups on GPUs without altering the model architecture or sacrificing accuracy. Despite their effectiveness, an alternative optimization focuses on extreme low-precision attention computation. Specifically, matrix multiplications with entries in binary representations can be efficiently implemented on modern hardware [35]. Therefore, developing an effective and hardware-friendly binary attention mechanism is an imperative demand to push the boundaries of the efficiency of Transformers.

In this paper, we theoretically analyze the feasibility of binary representations in attention computing and indicate that the essential similarity relationships can be preserved even in binary space. Building upon this insight, we present **BinaryAttention**, a novel quantization method that enables fast and accurate 1-bit qk-attention. We demonstrate the significant potential of 1-bit qk-attention for vision and diffusion transformers, achieving remarkable acceleration without compromising performance, as shown in Fig. 1. Specifically, we quantize attention queries and keys to 1-bit representations. This transforms the standard dot-product attention score into a distance-based and a direction-based mechanism, which can be computed with hyper-efficient bit-wise XNOR and popcount instructions. While this can drastically reduce the computational cost, relying solely on the similarity in binary space can cause the attention distribution to become overly uniform or flattened, as it discards the crucial magnitude information from the original tokens. To mitigate this flattened effect, we then introduce a learnable bias term, which is designed to be dense, position-sensitive, or context-aware, allowing expressive and discriminative 1-bit qk-attention. Furthermore, we design a hybrid quantization scheme that applies 8-bit precision to the attention weights and values, enabling end-to-end acceleration. Finally, to address the inherent approximation errors and the distribution shift caused by 1-bit quantization, we employ quantization-aware training (QAT) [36] and self-distillation [34] techniques to guide the model learning binary representations whose similarity aligns closely with their full-precision counterparts.

By adapting the hardware acceleration method of FlashAttention2 [13] into our BinaryAttention kernel, we achieve a more than 100% inference speedup over FlashAttention2 on A100 GPUs. We perform a comprehensive evaluation of BinaryAttention across vision transformers and diffusion transformers on fundamental vision tasks such as image

classification, detection, segmentation, and image generation. The results demonstrate that BinaryAttention consistently achieves or even exceeds the performance of its full-precision attention counterparts. Our work establishes a significantly efficient and effective alternative to full-precision attention, largely advancing the development of efficient transformers for visual tasks.

2. Related Work

Attention architecture. In response to the quadratic complexity of attention in Transformers, there have been significant attempts in redesigning the computation architecture of attentions, including linear attention [2, 37, 76, 82, 84], sparse attention [3, 21, 63, 69, 78, 85], and state space models [14, 23, 25]. Linear attention reformulates the computing process of attention to achieve linear complexity. For instance, Katharopoulos *et al.* [37] replaced the softmax operation with carefully designed kernel functions. Wang *et al.* [76] proposed Linformer, which adopts an alternative design that approximates the attention computation using low-rank matrix factorization. Yang *et al.* [82] generalized linear attention based on the gated delta rule, allowing more expressive variants while maintaining linear complexity. Sparse attention approaches reduce the complexity by limiting interactions to strategically selected token pairs, encompassing common designs such as sliding window [3, 63], sink [69, 78] and hybrid [21, 85] patterns. Recently, state space models (SSMs) [14, 23, 24, 54, 91] have emerged to replace attention with efficient recurrent scanning processes. Models like Mamba [14, 23] demonstrated that SSMs achieve Transformer-like capability with linear complexity.

Quantization techniques. Quantization techniques reduce model precision to achieve acceleration, which can be divided into two categories: post-training quantization (PTQ) [20, 46, 50, 87–89] minimizes quantization error without retraining, and quantization-aware training (QAT) [31, 39, 44, 51, 79, 81] simulates the effects of quantization during the training or fine-tuning process. Frantar *et al.* [20] presented GPTQ, which quantizes weight parameters by leveraging second-order statistics. Lin *et al.* [46] developed AWQ, which protects salient weights by determining the per-channel scaling factors based on the distribution of activations. Several approaches have pushed the quantization to binary space specifically for vision transformers [31, 39, 79]. More recent efforts have extended quantization to the computation of attention. Zhang *et al.* [89] introduced SageAttention, which employs block-wise INT8 quantization for attention queries and keys. SageAttention2 [87] quantizes queries and keys to INT4 and computing the attention map and values in FP8. SageAttention3 [88] goes further by unifying the attention computations to FP4.

Hardware optimization. This strategy unleashes hardware capabilities to improve efficiency. Lefaudeux *et al.*

[40] developed xFormers, which optimizes attention through customized and memory-efficient CUDA kernels. Dao *et al.* [15] introduced the concept of IO-aware tiled attention and proposed FlashAttention, achieving significant speedups. FlashAttention2 [13] refines this through improved parallelism and warp-level partition. FlashAttention3 [65] further exploits Hopper GPU architecture by leveraging asynchronous communication and FP8 Tensor Core. Based on these developments, SageAttention [87–89] integrates FlashAttention with low-precision quantization, leading to significant gains in overall efficiency.

3. Preliminaries

Model quantization [22] aims to quantize the high-bit (*e.g.*, FP32) weights and activations of a network model into low-bit representations (*e.g.*, INT8) for efficient deployment. A simple approach is uniform quantization, which linearly maps the floating-point values to a discrete set of levels. For a given full-precision vector $\mathbf{x} \in \mathbb{R}^d$, this process can be described as: $\tilde{\mathbf{x}} = \lceil \mathbf{x}/s \rceil + z$, $\hat{\mathbf{x}} = s(\tilde{\mathbf{x}} - z)$, where $\tilde{\mathbf{x}}$ is the quantized value, $\lceil \cdot \rceil$ means rounding operation, s is a scaling factor, z is a zero point, and $\hat{\mathbf{x}}$ denotes the de-quantized value that approximates the original \mathbf{x} . An extreme case is binary quantization [57], which simplifies the approximation to $\hat{\mathbf{x}} = \alpha \text{sign}(\mathbf{x})$ with an optimal scaling factor α , where the element-wise function $\text{sign}(\mathbf{x})$ maps non-negative values to 1 and others to -1 .

Attention is the cornerstone of the Transformer architecture. Given an input $\mathbf{x} \in \mathbb{R}^{N \times d}$ of length N , single head softmax attention [74] computes output $\mathbf{y} \in \mathbb{R}^{N \times d}$ as:

$$\mathbf{y}_i = \sum_{j=1}^N \left(\frac{\exp(\mathbf{q}_i^T \mathbf{k}_j / \sqrt{d})}{\sum_{j=1}^N \exp(\mathbf{q}_i^T \mathbf{k}_j / \sqrt{d})} \right) \mathbf{v}_j = \sum_{j=1}^N P_{ij} \mathbf{v}_j, \quad (1)$$

where the query, key and value tokens ($\mathbf{q}_i, \mathbf{k}_j, \mathbf{v}_j \in \mathbb{R}^d$) are generated by projecting \mathbf{x} with learnable weight matrices. P_{ij} is the attention coefficient computed over $(\mathbf{q}_i, \mathbf{k}_j)$.

4. Binary Attention

4.1. Theoretical Motivation for Binary Attention

We commence by establishing a theoretical bridge between standard and binary attention, demonstrating the feasibility of our approach. As shown in Eq. (1), softmax attention computes a weighted sum over the values. The attention coefficient P_{ij} is determined by the dot-product similarity $S_{ij} = \mathbf{q}_i^T \mathbf{k}_j$ between query and key. This similarity can be interpreted from two complementary perspectives.

Suppose that the query \mathbf{q}_i and key \mathbf{k}_j are L_2 normalized, a common practice known as QKNorm [32]. With $\|\mathbf{q}_i - \mathbf{k}_j\|_2^2 = \|\mathbf{q}_i\|_2^2 + \|\mathbf{k}_j\|_2^2 - 2\mathbf{q}_i^T \mathbf{k}_j$, the attention coefficient

can be expressed as:

$$P_{ij} \propto \exp(-\|\mathbf{q}_i - \mathbf{k}_j\|_2^2 / \tau), \quad (2)$$

where τ is a scaling factor. This formulation reveals that softmax attention actually behaves as a distance-based metric in Euclidean space. Alternatively, the dot-product similarity can be rewritten as $\mathbf{q}_i \mathbf{k}_j^T = \|\mathbf{q}_i\|_2 \|\mathbf{k}_j\|_2 \cos \theta$, where θ refers to the angle between the query \mathbf{q}_i and key \mathbf{k}_j . With L_2 normalization, the attention coefficient is therefore proportional to the cosine similarity, scaled by τ :

$$P_{ij} \propto \exp(\cos \theta / \tau). \quad (3)$$

This shows that the attention mechanism can be interpreted as operating on the directional similarity.

With the above dual perspectives of standard attention in mind, we explore whether these relationships can be preserved under 1-bit quantization of it. We represent the binary counterparts of query \mathbf{q}_i and key \mathbf{k}_j as $\mathbf{s}_i = \text{sign}(\mathbf{q}_i), \mathbf{t}_j = \text{sign}(\mathbf{k}_j) \in \{-1, 1\}^d$, respectively. Then, the dot-product similarity can be expressed directly in terms of the Hamming distance as $S_{ij} = \mathbf{s}_i^T \mathbf{t}_j = d - 2\|\mathbf{s}_i - \mathbf{t}_j\|_H$, where the Hamming norm $\|\mathbf{x}\|_H$ is defined as the number of non-zero entries of \mathbf{x} . Thus, the attention coefficient is given by:

$$P_{ij} \propto \exp(-\|\mathbf{s}_i - \mathbf{t}_j\|_H / \tau). \quad (4)$$

This indicates that binary attention operates as a distance-based metric in the Hamming space, mirroring the Euclidean distance in standard attention. Beyond this, it also preserves the directional similarity. Since the dot-product $\mathbf{s}_i^T \mathbf{t}_j$ in binary domain equals $d \cos \theta$, the attention coefficient can be equivalently expressed as $P_{ij} \propto \exp(\cos \theta / \tau)$.

While the above analyzes reveal the structural parallels between binary and standard attentions in their respective spaces, a more fundamental connection exists at the statistical level. We show that binary attention preserves the covariance structure of the original queries and keys, as shown in the following **Theorem 1**.

Theorem 1. Consider two random variables $\mathbf{q}, \mathbf{k} \in \mathbb{R}^d$. Suppose that $\mathbf{z} = (\mathbf{q}^T, \mathbf{k}^T)^T \in \mathbb{R}^{2d}$ is a zero-mean Gaussian vector with covariance matrix Σ , where $\Sigma = \begin{bmatrix} \Sigma_{qq} & \Sigma_{qk} \\ \Sigma_{kq} & \Sigma_{kk} \end{bmatrix}$. Denote $D_q = \text{diag}(\Sigma_{qq}), D_k = \text{diag}(\Sigma_{kk})$ and $C = D_q^{-\frac{1}{2}} \Sigma_{qk} D_k^{-\frac{1}{2}}$. For any $\mathbf{s} = \text{sign}(\mathbf{q})$ and $\mathbf{t} = \text{sign}(\mathbf{k})$, there is:

$$\mathbb{E}[\mathbf{s} \mathbf{t}^T] = \frac{2}{\pi} \arcsin C.$$

Proof. Please see **supplementary file** for the proof. \square

Theorem 1 implies that the outer product formed by binary queries and keys is a consistent estimate of the original

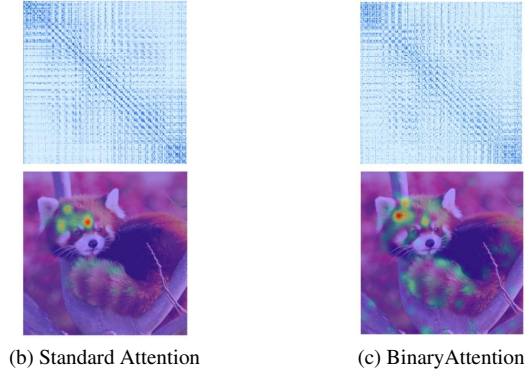
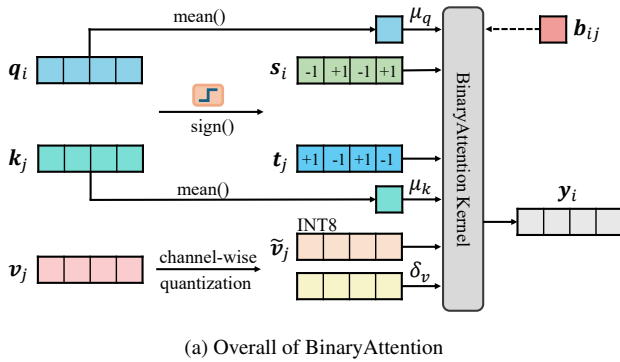


Figure 2. Overview and comparative analysis of BinaryAttention. (a) The computation of BinaryAttention involves three components: converting queries and keys into scaled binary representations, applying a bias enhancement, and quantizing the attention coefficients and values. Sub-figures (b) and (c) show the attention maps (top) and the corresponding activation maps (bottom) for Standard Attention and our BinaryAttention, demonstrating the comparable expressivity of BinaryAttention to Standard Attention despite 1-bit quantization.

covariance matrix. Crucially, the covariance matrix shares equivalent non-zero eigenspectrum with the Gram matrix, which contains all pairwise dot products between queries and keys and governs the core relational structure of standard attention. Theorem 1 provides a guarantee for the performance of binary attention, ensuring its expressive capability.

4.2. Formulation of BinaryAttention

We now propose BinaryAttention, an effective 1-bit qk-attention method. As illustrated in Fig. 2(a), BinaryAttention comprises the following three key components.

Scaled binary representations. The primary computational bottleneck in standard attention lies in the floating-point matrix multiplication between queries and keys. To address this, we replace this expensive operation with a highly efficient binary alternative. Specifically, we first quantize the query q_i and key k_j into binary values via a scaled 1-bit quantization function:

$$s_i = \mu_q \text{sign}(q_i), \quad t_j = \mu_k \text{sign}(k_j), \quad (5)$$

where $\mu_q, \mu_k \in \mathbb{R}_{\geq 0}$ are the means of queries and keys along the token and channel axes, respectively. The dot-product similarity S_{ij} is computed as $\mu_q \mu_k s_i^T t_j$ in binary space, which is not only statistically aligned with its full-precision counterpart but also extremely efficient by leveraging bit-wise XNOR and popcount instructions.

Bias enhancement. While computationally efficient, the 1-bit quantization of queries and keys introduces two challenges that can degrade attention performance: a loss of magnitude information and a subsequent distribution shift in the attention scores. The binary representations project data of varying scales onto the unit hyper-sphere, sacrificing the nuanced relationships captured by the original full-precision dot products. Consequently, the softmax distribution in binary space tends to produce overly uniform attention coefficients that are difficult to distinguish salient features. To

counteract this, we introduce a bias term as follows:

$$S_{ij} = \mu_q \mu_k s_i^T t_j / \sqrt{d} + b_{ij}, \quad (6)$$

where $b_{ij} \in \mathbb{R}$ is an optional bias that can be tailored to different scenarios and architectures. For instance, the bias can be a dense learnable matrix to increase the rank of dot-product similarities in binary space. Alternatively, it can be instantiated as position-sensitive or context-aware to explicitly model spatial structural and context-specific priors.

The bias term acts as a corrective measure, reintroducing the contextual or structural information back into the computation of attention coefficients, effectively avoiding the collapse of the attention distribution and enabling BinaryAttention to capture complex and long-range dependencies that are critical for visual tasks.

Quantization of attention coefficients and values. To achieve a holistic acceleration of the entire attention computation, we further extend the low-bit computation to the attention coefficients and the values, which are primarily memory-bound. To address this, BinaryAttention pairs the dot-product similarities in binary space with specific 8-bit quantization schemes tailored to these two components. For the attention coefficients P_{ij} , which is naturally constrained to the range $[0, 1]$ by the softmax operation, we employ an unsigned 8-bit quantization with a static scale of $1/255$. For the value v_j , which typically exhibits more complex statistical distributions with potential outliers across channels, we adopt a channel-wise 8-bit quantization strategy with a scale δ_v . The quantization process and subsequent value aggregation are formulated as:

$$\tilde{P}_{ij} = \lceil P_{ij} \times 255 \rceil, \quad \tilde{v}_j = \lceil v_j / \delta_v \rceil, \quad y_i = \sum_{j=1}^N \frac{\delta_v}{255} \tilde{P}_{ij} \tilde{v}_j. \quad (7)$$

Here, \tilde{P}_{ij} and \tilde{v}_j denote the quantized 8-bit integers. This

design enables efficient integer operations while maintaining the accuracy through proper scaling factors.

Remark. The BinaryAttention framework, through its three core components, achieves a balance between computational efficiency and representation capabilities. The scaled binary representations enable hardware-friendly computation, the optional bias recovers discriminative ability, and the hybrid quantization ensures end-to-end acceleration. As shown in Fig. 2(b) and 2(c), the attention and activation maps from BinaryAttention reveal strikingly similar patterns with those from standard attention, focusing on analogous related regions with a high correlation. This alignment demonstrates that, even under extreme 1-bit quantization, BinaryAttention retains the content-based dynamic routing and long-range dependencies modeling capabilities of standard attention.

4.3. Hardware-Aware Implementation

We take advantage of the capabilities of modern GPU hardware to implement BinaryAttention, building upon the foundational principles of FlashAttention2 [13] while introducing dedicated optimizations. The complete algorithm is detailed as Algorithm 1 in **supplementary file**. In particular, we utilize the fast `mma.s32.b1.b1.s32` PTX instruction (referred to as ‘BinaryMatmul’ in Algorithm 1) of NVIDIA Tensor Cores for the similarity computations between binary queries and keys. For the attention coefficients and values multiplications, we employ the `mma.s32.u8.s8.s32` instruction (referred to as ‘IntMatmul’ in Algorithm 1), which is optimized for mixed-precision 8-bit matrix operations.

Our implementation maintains the memory hierarchy optimizations and block tiling strategies of FlashAttention2 [13], but adapts them specifically for the binary and low-precision context. This hardware-aware design ensures that BinaryAttention delivers practical speedups through extreme quantization of attention computation.

5. Experimental Results

We conduct extensive experiments to evaluate the efficiency and effectiveness of BinaryAttention. Our primary competitors are FlashAttention2 [13] and SageAttention [89], which share the same objective as BinaryAttention, *i.e.*, accelerating the computation of standard attention. While linear attention [5, 7, 27, 28, 66, 83] and SSMs [54, 91] also improve efficiency, they address the quadratic complexity problem by significantly changing the computing architecture of attention, which are actually orthogonal to our work. In addition, traditional model quantization methods [45, 86] mainly target linear layers rather than attention computations. Therefore, they are also complementary to our work.

In the following experiments, we take FlashAttention2 as the baseline to implement our method.

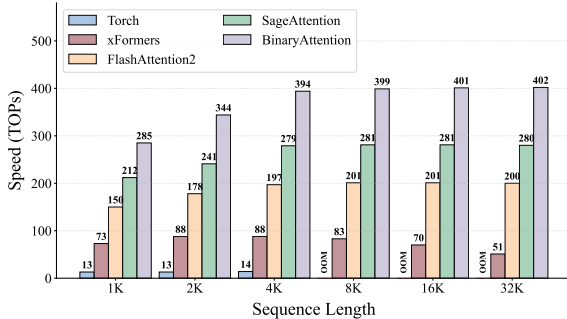


Figure 3. Kernel speed comparison on A100 GPUs.

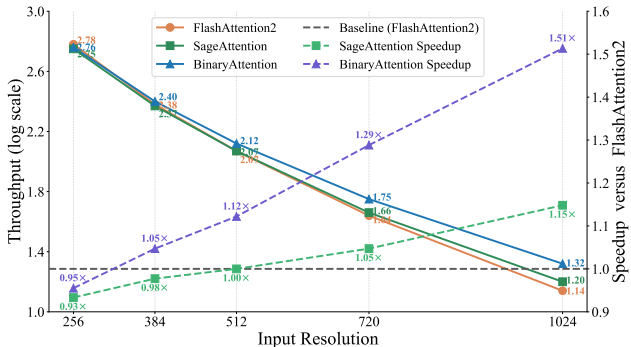


Figure 4. End-to-end throughput and speedup comparisons on A100 GPUs. ViT [18] models are used.

5.1. Efficiency Comparison

The two matrix multiplications dominate standard attention computation: the interaction between queries and keys (QK^T) and the aggregation of values (PV). The acceleration of BinaryAttention comes from the massive throughput advantages of low-precision arithmetic on modern hardware. Specifically, NVIDIA A100 Tensor Cores offer theoretical throughput of 312 TFLOPs/s for FP16, 624 TFLOPs/s for INT8, and an impressive 4992 TOPs/s for binary operations. By implementing QK^T with binary representations and PV with INT8 quantization, BinaryAttention achieves theoretical speedups of 16 \times and 2 \times for these computations, respectively, yielding an overall theoretically 3.5 \times improvement for standard FP16 attention implementation.

In practice, acceleration performance is constrained by memory bandwidth and I/O limitations. We benchmark the efficiency of BinaryAttention with several attention implementations, including Torch [55], xFormers [40], FlashAttention2 [13], and SageAttention [89]. Fig. 3 shows the kernel speed across varying sequence lengths with a head dimension of 128 on A100 GPUs. It can be seen that BinaryAttention consistently outperforms all competing methods. Specifically, it is about 2 \times and 1.4 \times faster than FlashAttention2 and SageAttention, respectively.

Moreover, we perform end-to-end inference and evaluate the log-scaled throughput on ViT [18] models with a

patch size of 8, as presented in Fig. 4. While our method and SageAttention slightly slower than FlashAttention2 at low resolutions due to quantization overheads, BinaryAttention significantly outperforms all methods at higher resolutions, achieving a $1.5\times$ speedup over FlashAttention2 and $1.3\times$ over SageAttention at 1024×1024 inputs. This further demonstrates that our BinaryAttention is compatible to modern hardware to achieve higher efficiency.

5.2. Image Classification

Settings. We first evaluate the image classification task using ImageNet-1K [16]. Following DeiT [72], we develop three variants of BinaryAttention, namely -T (tiny), -S (small) and -B (base), by substituting all standard attention modules with BinaryAttention. We follow the experimental settings in DeiT [72], which are detailed in **supplementary file**. The models are fine-tuned with the self-distillation [34] strategy, where the full-precision counterparts serve as the teacher.

We compare with quantization based methods PTQ4ViT [86] (W8A8), I-ViT [45] (W8A8) and the attention quantization method SageAttention [89]. We also compare with Linear Transformers [5, 7, 27, 28, 66, 83] and SSMs [54, 91] for reference. Following [31, 61], we count binary operations (BOPs) and floating-point operations (FLOPs) separately and report the total operations (OPs) as $OPs=BOPs/64+FLOPs$.

Results. Tab. 1 presents the comparison result. BinaryAttention demonstrates consistent performance advantages in multiple dimensions. Compared with the baseline DeiT (implemented with FlashAttention2) and the recent SageAttention, BinaryAttention achieves higher accuracy with reduced computational cost. For instance, BinaryAttention-T attains a top-1 accuracy of 72.88%, outperforming DeiT-T by 0.68% and SageAttention-T by 0.77% with fewer OPs. BinaryAttention-S and BinaryAttention-B achieve top-1 accuracies of 80.24% and 82.04% at a resolution of 224×224 , surpassing SageAttention by 0.42% and 0.21%, respectively. Notably, at higher resolution 384×384 , BinaryAttention-B achieves the highest accuracy of 83.64% with 50.2G OPs, demonstrating superior performance to DeiT-B (83.1%, 55.4G OPs) and SageAttention-B (82.89%, 53.2G OPs).

Compared with W8A8 quantization methods, BinaryAttention delivers superior accuracy albeit requires more OPs. BinaryAttention-T costs 1.1G OPs, higher than PTQ4ViT-T (0.3G OPs), but achieves much higher accuracy (72.88% vs. 71.6%). Note that BinaryAttention can be seamlessly integrated with these quantization techniques for linear layers. Both BinaryAttention and SageAttention can achieve a substantial reduction in OPs when combined with PTQ4ViT, but BinaryAttention maintains high accuracy. Specifically, BinaryAttention-B+PTQ4ViT holds a top-1 accuracy of 83.55% with only 13.5G OPs, which is 0.57% higher than SageAttention-B+PTQ4ViT with 3G fewer OPs.

We also include Linear Transformers and SSMs in the

	Method	Reso.	#Param.	OPs	Top-1	
Linear Transformer	Hydra-T [5]	224^2	6M	1.1G	68.3	
	Efficient-T [66]	224^2	6M	1.1G	70.2	
	Angular-T [83]	224^2	6M	1.1G	70.8	
	Enhanced-T [7]	224^2	6M	1.1G	72.9	
	FLatten-T [27]	224^2	6M	1.1G	74.1	
	InLine-T [28]	224^2	7M	1.1G	74.5	
	InLine-S	288^2	17M	5.0G	80.2	
InLine-B	448^2	24M	17.2G	82.3		
SSM	S4ND-ViT-B [54]	224^2	89M	-	80.4	
	Vim-T [91]	224^2	7M	1.5G	76.1	
	Vim-S	224^2	26M	5.1G	80.3	
	Vim-B	224^2	98M	18.9G	81.9	
Transformer	DeiT-T [72]	224^2	6M	1.2G	72.2	
	DeiT-S	224^2	22M	4.6G	79.8	
	DeiT-B	224^2	87M	17.6G	81.8	
	DeiT-B	384^2	87M	55.4G	83.1	
	W8A8 Quantization					
	PTQ4ViT-T [86]	224^2	6M	0.3G	71.6	
	PTQ4ViT-S	224^2	22M	1.2G	79.5	
	PTQ4ViT-B	224^2	87M	4.5G	81.5	
	PTQ4ViT-B	384^2	87M	14.2G	83.0	
	I-ViT-T [45]	224^2	6M	0.3G	72.2	
	I-ViT-S	224^2	22M	1.2G	80.1	
	I-ViT-B	224^2	87M	4.5G	81.7	
	Attention Quantization					
	SageAttention-T [89]	224^2	6M	1.2G	72.11	
	+PTQ4ViT	224^2	6M	0.4G	71.63	
	SageAttention-S	224^2	22M	4.5G	79.82	
	+PTQ4ViT	224^2	22M	1.3G	79.38	
	SageAttention-B	224^2	87M	17.3G	81.83	
	+PTQ4ViT	224^2	87M	4.8G	81.58	
	SageAttention-B	384^2	87M	53.2G	82.89	
+PTQ4ViT	384^2	87M	16.5G	82.98		
BinaryAttention-T	224^2	6M	1.1G	72.88		
+PTQ4ViT	224^2	6M	0.3G	72.61		
BinaryAttention-S	224^2	22M	4.3G	80.24		
+PTQ4ViT	224^2	22M	1.2G	79.81		
BinaryAttention-B	224^2	87M	17.0G	82.04		
+PTQ4ViT	224^2	87M	4.4G	81.91		
BinaryAttention-B	384^2	87M	50.2G	83.64		
+PTQ4ViT	384^2	87M	13.5G	83.55		

Table 1. Comparison of image classification on ImageNet-1K.

comparison just for reference. While Flatten-T, InLine-T, and Vim-T achieve higher accuracy in some configurations, they struggle to scale up effectively. InLine-S/B relies on larger input and Vim-S/B requires significantly more parameters and OPs. In contrast, BinaryAttention maintains robust performance without architecture changes.

The comprehensive evaluations presented above highlight the effectiveness of BinaryAttention in maintaining the expressive capability of standard attention while achieving substantial efficiency improvement.

(a) Mask R-CNN														
Backbone	AP ^b	AP ^b ₅₀	AP ^b ₇₅	AP ^b _s	AP ^b _m	AP ^b _l	AP ^m	AP ^m ₅₀	AP ^m ₇₅	AP ^m _s	AP ^m _m	AP ^m _l	#Param.	OPs
DeiT-T	41.11	62.24	44.71	23.50	44.00	56.56	37.26	59.20	39.63	17.35	39.55	56.62	28M	338G
SageAttention-T	41.10	62.21	44.65	23.52	44.02	56.43	37.26	59.23	39.62	17.39	39.57	56.61	28M	327G
BinaryAttention-T	41.29	62.04	44.91	23.99	44.62	55.81	37.26	59.10	39.68	17.71	39.89	55.85	28M	313G
DeiT-S	45.49	67.29	49.10	28.91	48.56	61.57	40.87	63.90	43.57	21.95	43.56	60.89	44M	440G
SageAttention-S	45.48	67.23	49.13	28.87	48.65	61.62	40.85	63.90	43.59	21.92	43.52	60.86	44M	418G
BinaryAttention-S	45.86	67.29	49.77	30.03	49.16	61.72	41.01	64.10	43.68	22.39	43.71	60.34	44M	390G
DeiT-B	47.99	69.46	52.07	31.59	51.11	64.04	42.98	66.48	46.29	23.82	45.64	61.85	111M	785G
SageAttention-B	47.97	69.46	52.08	31.64	51.13	63.97	42.99	66.50	46.29	23.82	45.65	61.83	111M	742G
BinaryAttention-B	48.28	69.98	52.58	31.96	51.68	63.44	43.24	66.75	46.44	24.60	46.10	61.03	111M	685G

(b) Cascade Mask R-CNN														
Backbone	AP ^b	AP ^b ₅₀	AP ^b ₇₅	AP ^b _s	AP ^b _m	AP ^b _l	AP ^m	AP ^m ₅₀	AP ^m ₇₅	AP ^m _s	AP ^m _m	AP ^m _l	#Param.	OPs
DeiT-T	46.39	64.58	50.11	27.05	50.03	63.71	39.90	61.75	42.91	19.37	42.75	59.73	58M	595G
SageAttention-T	46.45	64.59	50.10	27.11	50.09	63.70	39.91	61.70	42.90	19.39	42.73	59.68	58M	584G
BinaryAttention-T	46.64	64.79	50.37	28.07	50.24	63.14	40.12	62.00	43.05	20.54	42.94	59.46	58M	570G
DeiT-S	49.44	68.10	53.16	32.01	53.20	65.18	42.52	65.12	45.90	23.32	45.40	60.89	75M	696G
SageAttention-S	49.46	68.16	53.20	32.07	53.22	65.14	42.51	65.13	45.93	23.41	45.38	60.88	75M	675G
BinaryAttention-S	49.63	68.00	53.65	32.83	53.00	65.70	42.72	65.42	46.09	23.80	45.23	61.37	75M	647G
DeiT-B	50.21	68.63	54.53	33.29	53.43	65.56	43.49	66.25	47.05	24.69	46.03	61.05	141M	1041G
SageAttention-B	50.20	68.62	54.55	33.29	53.39	65.58	43.48	66.27	47.06	24.55	45.98	61.06	141M	999G
BinaryAttention-B	50.16	68.80	54.09	32.90	53.31	66.26	43.49	66.28	47.15	24.28	46.17	62.23	141M	941G

Table 2. Comparison of object detection and instance segmentation on COCO. OPs are computed with input resolution of 1024×1024.

Backbone	Crop size	mIoU (SS)	mIoU (MS)	#Param.	OPs
DeiT-T	512 ²	39.82	40.68	11M	227G
SageAttention-T	512 ²	39.82	40.68	11M	198G
BinaryAttention-T	512 ²	39.93	40.89	11M	159G
DeiT-S	512 ²	44.67	46.01	43M	744G
SageAttention-S	512 ²	44.67	46.01	43M	687G
BinaryAttention-S	512 ²	44.75	45.95	43M	610G
DeiT-B	512 ²	46.86	47.74	166M	2654G
SageAttention-B	512 ²	46.86	47.74	166M	2539G
BinaryAttention-B	512 ²	47.76	48.37	166M	2384G

Table 3. Comparison of semantic segmentation on ADE20K. ‘SS’ and ‘MS’ represent single-scale and multi-scale testing, respectively. OPs are calculated with input resolution of 512 × 2048.

5.3. Object Detection and Instance Segmentation

Settings. We then evaluate object detection and instance segmentation tasks with COCO 2017 dataset [47] and Detectron2 [77] library. Following ViTDet [43], we apply Mask R-CNN [29] and Cascade Mask R-CNN [8] as detector heads, with ImageNet-1K pre-trained BinaryAttention-T/S/B as backbones. During training, we employ the AdamW optimizer with beta set to (0.9, 0.999), momentum of 0.9 and a batch size of 64. The initial learning rate is set to 0.001 with a weight decay of 0.1. A linear learning rate decay is adopted with a warm-up of 250 iterations.

Results. The results are reported in Tab. 2. BinaryAttention shows competitive performance with lower computational cost. For the Mask R-CNN head, BinaryAttention-T achieves 0.18 higher box mAP than DeiT-T with the same mask mAP of 37.26, while reducing OPs by 25G compared to DeiT-T and 14G to SageAttention-T. BinaryAttention-S exceeds DeiT-S by 0.37 in box mAP and 0.14 in mask mAP, with significant gains on small-size objects, from 28.87 to 30.03 in small box mAP. BinaryAttention-B maintains the superior performance to DeiT-B, while performing slightly lower in large-size objects. Similar observations can be made in the Cascade Mask R-CNN head. BinaryAttention-T and -S achieve consistent gains over their DeiT counterparts, with -S reaching a box mAP of 49.63 and a mask mAP of 42.72. Furthermore, BinaryAttention-B delivers a more favorable accuracy and efficiency trade-off, matching its full-precision counterpart with a 10% reduction in OPs.

5.4. Semantic Segmentation

Settings. We further evaluate BinaryAttention on semantic segmentation using ADE20K [90] and MMsegmentation [12]. Following [19], we adopt the widely used UPerNet [80] as the segmenter and our pre-trained models as backbones. We train the models for 60K iterations with a batch size of 32, using the AdamW optimizer with a weight decay of 0.01, and an initial learning rate of 6×10^{-5} with a linear learning rate decay, following a warm-up of 1500 iterations.

Results. As shown in Tab. 3, BinaryAttention achieves im-

Method	OPs	Steps	FID↓	sFID↓	IS↑	Pre.↑	Re.↑	FID↓	sFID↓	IS↑	Pre.↑	Re.↑
(cfg=1.25)			DiT-S/2					SiT-S/2				
FlashAttention2	6.1G	400K	54.73	10.21	26.83	0.42	0.57	46.33	7.89	31.99	0.46	0.59
SageAttention	5.8G	400K	54.74	10.21	26.86	0.42	0.57	46.32	7.89	32.00	0.46	0.59
BinaryAttention	5.5G	200K	49.76	10.40	30.14	0.45	0.57	41.40	7.99	36.49	0.48	0.59
(cfg=1.50)			DiT-S/2					SiT-S/2				
FlashAttention2	6.1G	400K	43.87	8.82	35.16	0.48	0.55	36.26	7.09	42.24	0.52	0.56
SageAttention	5.8G	400K	43.90	8.82	35.19	0.48	0.55	36.25	7.09	42.25	0.52	0.56
BinaryAttention	5.5G	200K	38.96	8.95	40.12	0.50	0.56	31.18	7.12	50.54	0.55	0.56
(cfg=1.25)			DiT-XL/2					SiT-XL/2				
FlashAttention2	118.6G	7000K	3.22	5.28	201.77	0.76	0.62	3.62	5.23	193.51	0.75	0.64
SageAttention	117.1G	7000K	3.24	5.29	201.72	0.76	0.62	3.68	5.25	191.57	0.75	0.64
BinaryAttention	115.0G	4000K	4.26	6.33	199.59	0.72	0.65	4.22	5.74	191.57	0.74	0.65
(cfg=1.50)			DiT-XL/2					SiT-XL/2				
FlashAttention2	118.6G	7000K	2.27	4.60	278.24	0.83	0.57	2.15	4.60	258.09	0.81	0.60
SageAttention	117.1G	7000K	2.27	4.59	278.03	0.83	0.58	2.16	4.63	256.07	0.80	0.61
BinaryAttention	115.0G	4000K	2.19	5.01	278.03	0.80	0.61	2.21	4.89	250.02	0.79	0.61

Table 4. Comparison of class-conditional image generation on ImageNet 256×256.



Figure 5. Qualitative comparison of generated image by DiT-XL/2 (cfg=1.50) using FlashAttention2 and BinaryAttention.

pressive performance on the semantic segmentation task. For instance, BinaryAttention-T achieves a single-scale mIoU of 39.93 and a multi-scale mIoU of 40.89 with fewer OPs, outperforming DeiT-T by 0.11 and 0.21 mIoU, respectively. BinaryAttention-S is slightly higher than DeiT-S in single-scale mIoU and nearly identical to the baseline in multi-scale testing. BinaryAttention-B delivers a considerable improvement, achieving 47.76 single-scale mIoU and 48.37 multi-scale mIoU, exceeding DeiT-B by 0.90 and 0.63 mIoU, respectively, while reducing computational cost by 270G OPs. These results confirm that BinaryAttention excels at complex scene understanding while preserving the fine-grained details essential for semantic segmentation.

5.5. Image Generation

Settings. Finally, we explore the applicability of BinaryAttention to class-conditional image generation task. Following Diffusion Transformers (DiT) [56] and Scalable Interpolant Transformers (SiT) [52], we replace their standard attention modules with our BinaryAttention. We train all models on ImageNet at 256 × 256 image resolution, with 200K iter-

ations for small-size models and 4000K for XL variants, using the original training configurations without any hyperparameter changes. The models are initialized with the pre-trained DiT and SiT models. During evaluation, we generate 50K images using 250 sampling steps, applying the DDPM scheduler to DiT and the ODE solver to SiT. Fréchet Inception Distance (FID) [33], sliding FID (sFID) [53], Inception Score (IS) [64] and Precision and Recall [38] are used to evaluate the generative performance.

Results. The results are summarized in Tab. 4. For DiT-S/2 and SiT-S/2 models, BinaryAttention shows substantial improvements over both FlashAttention2 and SageAttention while having fewer OPs. It achieves significantly better FID with different classifier-free guidance (cfg) scales than the baseline models at 400K steps. It also demonstrates higher IS and Precision. For XL models, BinaryAttention shows slightly lower performance when using a smaller cfg scale at 4000K steps, but it matches or even exceeds FlashAttention2 and SageAttention with a higher cfg (1.50), achieving the lowest FID of 2.19 for DiT-XL/2. Qualitative comparison in Fig. 5 further demonstrates that BinaryAttention achieves a generation quality on par with full-precision models, producing images that are detailed and structurally consistent.

5.6. Ablation Study

We first conduct a series of ablation studies to analyze the core components of BinaryAttention, including scaled binary representations, bias enhancement, and the self-distillation strategy. The experiments are performed on the ImageNet-1K [16] benchmark by using DeiT [72] architectures. The results are summarized in Tab. 5.

Scaled Binary Representations. We evaluate the role of scaling factors in binary representations. When scaling is not

Scale	Bias	Distillation	DeiT-T Top-1	DeiT-S Accuracy	DeiT-B
Baseline (full-precision)			72.2	79.8	81.8
✗	✗	✗	71.95	79.59	81.10
✓	✗	✗	72.42	79.81	81.33
✓	✗	✓	72.44	79.97	81.99
✓	✓	✓	72.88	80.24	82.04

Table 5. Ablation studies on BinaryAttention for the scaled binary representations, bias enhancement and self-distillation strategy on ImageNet-1K benchmark, using DeiT architectures.

	CosSim	Relative L1	RMSE	Precision
Layer (0)	0.9186	0.4840	0.4165	0.7716
Layer (6)	0.8740	0.7353	0.5084	0.7301

Table 6. Attention pattern comparison between FlashAttention2 and BinaryAttention by DeiT-B on ImageNet-1K validation set.

applied, BinaryAttention shows performance drop across all models, with top-1 accuracy decreased by -0.25% , -0.21% , and -0.70% for DeiT-T, -S, and -B, respectively. Introducing scaling factors effectively solves this issue by minimizing the quantization error, with DeiT-T even exceeding its full-precision baseline (72.42% vs. 72.2%), demonstrating that proper scaling is essential for preserving representational capabilities in binary space.

Bias Enhancement. We simply employ a learnable relative position bias [49] as the bias term, which exhibits distinct effects across model scales. It provides an accuracy gain of 0.44% and 0.27% for DeiT-T and -S, respectively, while offering a slight improvement for DeiT-B, from 81.99% to 82.04%. This discrepancy stems from the relationship between model capacity and the expressive power of binary representations. For smaller models, the limited dimension constrains the diversity of attention patterns, making them more susceptible to distribution collapse. The bias term effectively mitigates this by introducing additional contextual or structural information. For larger models, higher-dimensional binary representations naturally preserve richer similarity structures, yielding more modest gains.

Self-distillation Strategy. We investigate the role of self-distillation, which slightly improves DeiT-T and -S models but significantly boosts the accuracy of DeiT-B by 0.66%. This improvement suggests that self-distillation effectively counteracts the distribution shift introduced by quantization errors while encouraging sign-aligned similarity between binary representations and its full-precision counterparts.

Attention Pattern Fidelity. We further analyze whether BinaryAttention preserves the original attention dynamics. We use Cosine Similarity, Relative L1 Distance, RMSE, and Precision as evaluation metrics, where Precision measures the

Method	Top-1	Mem. (512)	Mem. (1024)
FlashAttention2	72.2	1705M	5304M
SageAttention	72.11	1705M	5304M
BinaryAttention (den.)	72.88	3246M	29904M
BinaryAttention (dec.)	72.97	1706M	5307M

Table 7. Memory comparison by DeiT-T using FlashAttention2, SageAttention and BinaryAttention at resolutions of 512 and 1024.

FlashAttention2	SageAttention	BinaryAttention	Quant Q&K	Quant V
175.3ms	124.6ms	88.2ms	2.8ms	1.9ms

Table 8. Latency of attention kernels and quantization components measured on A100 GPUs.

accuracy of matching the top 100 most attended tokens. As shown in Tab. 6, BinaryAttention maintains high consistency with full-precision attention on ImageNet-1K validation set, with cosine similarity above 0.87 and precision around 0.75, demonstrating that BinaryAttention effectively preserves key relational patterns and structural relationships.

Memory and Quantization Overhead. Finally, we report the memory footprint in Tab. 7 and the quantization overhead in Tab. 8. BinaryAttention incurs extra memory primarily from the bias term. With a dense bias, memory grows rapidly with resolution, and with a decomposable bias, *e.g.*, a sum over spatial directions, the overhead becomes almost negligible. Meanwhile, the quantization cost is modest, requiring 2.8ms for query and key and 1.9ms for value (4.7ms in total), which accounts for about 5% of the BinaryAttention kernel.

6. Conclusion

We presented BinaryAttention, a simple yet accurate and efficient 1-bit qk-attention for vision and diffusion transformers. By establishing theoretical guaranties that token similarity persists in binary space, we incorporated scaled binary representations, bias enhancement, and hybrid quantization into standard attention, achieving $2\times$ speedup over FlashAttention2. Extensive experiments on image classification, detection, segmentation and generation validated that BinaryAttention matched or even surpassed full-precision attention with only 1-bit representations, demonstrating its strong potential for implementing ultra-low-precision inference deployment in practical vision tasks without compromising performance.

Limitations. Despite significant acceleration for computing QK^T similarity, the PV multiplications employ more conservative quantization, leaving room for greater end-to-end efficiency. Furthermore, our method currently focuses on optimizing attention computations specifically, leaving the complementary potential of jointly quantizing other components like MLP layers for future investigation.

References

- [1] Josh Achiam, Steven Adler, Sandhini Agarwal, Lama Ahmad, Ilge Akkaya, Florencia Leoni Aleman, Diogo Almeida, Janko Altenschmidt, Sam Altman, Shyamal Anadkat, et al. GPT-4 technical report. *arXiv preprint arXiv:2303.08774*, 2023. 1
- [2] Simran Arora, Sabri Eyuboglu, Michael Zhang, Aman Timalsina, Silas Alberti, James Zou, Atri Rudra, and Christopher Ré. Simple linear attention language models balance the recall-throughput tradeoff. In *Proceedings of the 41st International Conference on Machine Learning*, pages 1763–1840, 2024. 1, 2
- [3] Iz Beltagy, Matthew E Peters, and Arman Cohan. Longformer: The long-document transformer. *arXiv preprint arXiv:2004.05150*, 2020. 1, 2
- [4] Yoshua Bengio, Nicholas Léonard, and Aaron Courville. Estimating or propagating gradients through stochastic neurons for conditional computation. *arXiv preprint arXiv:1308.3432*, 2013. 15
- [5] Daniel Bolya, Cheng-Yang Fu, Xiaoliang Dai, Peizhao Zhang, and Judy Hoffman. Hydra Attention: Efficient attention with many heads. In *Computer Vision – ECCV 2022 Workshops*, pages 35–49, Cham, 2023. Springer Nature Switzerland. 5, 6
- [6] Tom Brown, Benjamin Mann, Nick Ryder, Melanie Subbiah, Jared D Kaplan, Prafulla Dhariwal, Arvind Neelakantan, Pranav Shyam, Girish Sastry, Amanda Askell, et al. Language models are few-shot learners. In *Advances in Neural Information Processing Systems*, pages 1877–1901, 2020. 1
- [7] Han Cai, Chuang Gan, and Song Han. EfficientViT: Enhanced linear attention for high-resolution low-computation visual recognition. *arXiv preprint arXiv:2205.14756*, 2022. 5, 6
- [8] Zhaowei Cai and Nuno Vasconcelos. Cascade R-CNN: Delving into high quality object detection. In *Proceedings of the IEEE Conference on Computer Vision and Pattern Recognition*, pages 6154–6162, 2018. 7
- [9] Jianfei Chen, Yu Gai, Zhewei Yao, Michael W Mahoney, and Joseph E Gonzalez. A statistical framework for low-bitwidth training of deep neural networks. In *Advances in Neural Information Processing Systems*, pages 883–894, 2020. 1
- [10] Bowen Cheng, Ishan Misra, Alexander G Schwing, Alexander Kirillov, and Rohit Girdhar. Masked-attention mask transformer for universal image segmentation. In *Proceedings of the IEEE/CVF Conference on Computer Vision and Pattern Recognition*, pages 1290–1299, 2022. 1
- [11] Aakanksha Chowdhery, Sharan Narang, Jacob Devlin, Maarten Bosma, Gaurav Mishra, Adam Roberts, Paul Barham, Hyung Won Chung, Charles Sutton, Sebastian Gehrmann, et al. PaLM: Scaling language modeling with pathways. *Journal of Machine Learning Research*, 24(240):1–113, 2023. 1
- [12] MMSegmentation Contributors. MMSegmentation: OpenMMLab semantic segmentation toolbox and benchmark. <https://github.com/open-mmlab/mms Segmentation>, 2020. 7
- [13] Tri Dao. FlashAttention-2: Faster attention with better parallelism and work partitioning. In *International Conference on Learning Representations*, 2024. 2, 3, 5, 14
- [14] Tri Dao and Albert Gu. Transformers are SSMs: Generalized models and efficient algorithms through structured state space duality. In *International Conference on Machine Learning*, 2024. 1, 2
- [15] Tri Dao, Daniel Y. Fu, Stefano Ermon, Atri Rudra, and Christopher Ré. FlashAttention: Fast and memory-efficient exact attention with IO-awareness. In *Advances in Neural Information Processing Systems*, pages 16344–16359, 2022. 1, 2, 3
- [16] Jia Deng, Wei Dong, Richard Socher, Li-Jia Li, Kai Li, and Li Fei-Fei. ImageNet: A large-scale hierarchical image database. In *2009 IEEE Conference on Computer Vision and Pattern Recognition*, pages 248–255. IEEE, 2009. 6, 8, 15
- [17] Jacob Devlin, Ming-Wei Chang, Kenton Lee, and Kristina Toutanova. BERT: Pre-training of deep bidirectional transformers for language understanding. In *North American Chapter of the Association for Computational Linguistics*, pages 4171–4186, 2019. 1
- [18] Alexey Dosovitskiy, Lucas Beyer, Alexander Kolesnikov, Dirk Weissenborn, Xiaohua Zhai, Thomas Unterthiner, Mostafa Dehghani, Matthias Minderer, Georg Heigold, Sylvain Gelly, Jakob Uszkoreit, and Neil Houlsby. An Image is Worth 16×16 Words: Transformers for image recognition at scale. In *International Conference on Learning Representations*, 2021. 1, 5
- [19] Yuxin Fang, Quan Sun, Xinggang Wang, Tiejun Huang, Xinlong Wang, and Yue Cao. EVA-02: A visual representation for neon genesis. *Image and Vision Computing*, 149:105171, 2024. 7
- [20] Elias Frantar, Saleh Ashkboos, Torsten Hoefler, and Dan Alistarh. GPTQ: Accurate post-training quantization for generative pre-trained transformers. *arXiv preprint arXiv:2210.17323*, 2022. 1, 2
- [21] Yizhao Gao, Zhichen Zeng, Dayou Du, Shijie Cao, Peiyuan Zhou, Jiaying Qi, Junjie Lai, Hayden Kwok-Hay So, Ting Cao, Fan Yang, et al. SeerAttention: Learning intrinsic sparse attention in your llms. *arXiv preprint arXiv:2410.13276*, 2024. 1, 2
- [22] Amir Gholami, Sehoon Kim, Zhen Dong, Zhewei Yao, Michael W Mahoney, and Kurt Keutzer. A survey of quantization methods for efficient neural network inference. In *Low-power Computer Vision*, pages 291–326. Chapman and Hall/CRC, 2022. 1, 3
- [23] Albert Gu and Tri Dao. Mamba: Linear-time sequence modeling with selective state spaces. In *First Conference on Language Modeling*, 2024. 1, 2
- [24] Albert Gu, Isys Johnson, Karan Goel, Khaled Saab, Tri Dao, Atri Rudra, and Christopher Ré. Combining recurrent, convolutional, and continuous-time models with linear state space layers. In *Advances in Neural Information Processing Systems*, pages 572–585, 2021. 2
- [25] Albert Gu, Karan Goel, and Christopher Ré. Efficiently modeling long sequences with structured state spaces. In *The International Conference on Learning Representations*, 2022. 1, 2
- [26] Daya Guo, Dejian Yang, Haowei Zhang, Junxiao Song, Ruoyu Zhang, Runxin Xu, Qihao Zhu, Shirong Ma, Peiyi

- Wang, Xiao Bi, et al. DeepSeek-R1: Incentivizing reasoning capability in LLMs via reinforcement learning. *arXiv preprint arXiv:2501.12948*, 2025. 1
- [27] Dongchen Han, Xuran Pan, Yizeng Han, Shiji Song, and Gao Huang. Flatten Transformer: Vision transformer using focused linear attention. In *Proceedings of the IEEE/CVF International Conference on Computer Vision*, pages 5961–5971, 2023. 5, 6
- [28] Dongchen Han, Yifan Pu, Zhuofan Xia, Yizeng Han, Xuran Pan, Xiu Li, Jiwen Lu, Shiji Song, and Gao Huang. Bridging the Divide: Reconsidering softmax and linear attention. In *Advances in Neural Information Processing Systems*, pages 79221–79245, 2024. 5, 6
- [29] Kaiming He, Georgia Gkioxari, Piotr Dollár, and Ross Girshick. Mask R-CNN. In *Proceedings of the IEEE International Conference on Computer Vision*, pages 2961–2969, 2017. 7
- [30] Kaiming He, Xinlei Chen, Saining Xie, Yanghao Li, Piotr Dollár, and Ross Girshick. Masked autoencoders are scalable vision learners. In *Proceedings of the IEEE/CVF Conference on Computer Vision and Pattern Recognition*, pages 16000–16009, 2022. 1
- [31] Yefei He, Zhenyu Lou, Luoming Zhang, Jing Liu, Weijia Wu, Hong Zhou, and Bohan Zhuang. BiViT: Extremely compressed binary vision transformers. In *Proceedings of the IEEE/CVF International Conference on Computer Vision*, pages 5651–5663, 2023. 1, 2, 6, 15
- [32] Alex Henry, Prudhvi Raj Dachapally, Shubham Shantaram Pawar, and Yuxuan Chen. Query-Key normalization for transformers. In *Findings of the Association for Computational Linguistics: EMNLP 2020*, pages 4246–4253, 2020. 3
- [33] Martin Heusel, Hubert Ramsauer, Thomas Unterthiner, Bernhard Nessler, and Sepp Hochreiter. Gans trained by a two time-scale update rule converge to a local nash equilibrium. In *Advances in Neural Information Processing Systems*, 2017. 8
- [34] Geoffrey Hinton, Oriol Vinyals, and Jeff Dean. Distilling the knowledge in a neural network. *arXiv preprint arXiv:1503.02531*, 2015. 2, 6
- [35] Itay Hubara, Matthieu Courbariaux, Daniel Soudry, Ran El-Yaniv, and Yoshua Bengio. Binarized neural networks. In *Advances in Neural Information Processing Systems*, 2016. 2
- [36] Benoit Jacob, Skirmantas Kligys, Bo Chen, Menglong Zhu, Matthew Tang, Andrew Howard, Hartwig Adam, and Dmitry Kalenichenko. Quantization and training of neural networks for efficient integer-arithmetic-only inference. In *Proceedings of the IEEE Conference on Computer Vision and Pattern Recognition*, pages 2704–2713, 2018. 1, 2
- [37] Angelos Katharopoulos, Apoorv Vyas, Nikolaos Pappas, and François Fleuret. Transformers are RNNs: Fast autoregressive transformers with linear attention. In *International Conference on Machine Learning*, pages 5156–5165. PMLR, 2020. 1, 2
- [38] Tuomas Kynkäänniemi, Tero Karras, Samuli Laine, Jaakko Lehtinen, and Timo Aila. Improved precision and recall metric for assessing generative models. In *Advances in Neural Information Processing Systems*, 2019. 8
- [39] Phuoc-Hoan Charles Le and Xinlin Li. BinaryViT: Pushing binary vision transformers towards convolutional models. In *Proceedings of the IEEE/CVF Conference on Computer Vision and Pattern Recognition*, pages 4665–4674, 2023. 1, 2
- [40] Benjamin Lefaudeux, Francisco Massa, Diana Liskovich, Wenhan Xiong, Vittorio Caggiano, Sean Naren, Min Xu, Jieru Hu, Marta Tintore, Susan Zhang, Patrick Labatut, Daniel Haziza, Luca Wehrstedt, Jeremy Reizenstein, and Grigory Sizov. xFormers: A modular and hackable transformer modelling library. <https://github.com/facebookresearch/xformers>, 2022. 3, 5
- [41] Bo Li, Yuanhan Zhang, Dong Guo, Renrui Zhang, Feng Li, Hao Zhang, Kaichen Zhang, Peiyuan Zhang, Yanwei Li, Ziwei Liu, et al. LLaVA-OneVision: Easy visual task transfer. *arXiv preprint arXiv:2408.03326*, 2024. 1
- [42] Junnan Li, Dongxu Li, Silvio Savarese, and Steven Hoi. BLIP-2: Bootstrapping language-image pre-training with frozen image encoders and large language models. In *International Conference on Machine Learning*, pages 19730–19742. PMLR, 2023. 1
- [43] Yanghao Li, Hanzi Mao, Ross Girshick, and Kaiming He. Exploring plain vision transformer backbones for object detection. In *European Conference on Computer Vision*, pages 280–296. Springer, 2022. 7
- [44] Yanjing Li, Sheng Xu, Baochang Zhang, Xianbin Cao, Peng Gao, and Guodong Guo. Q-ViT: Accurate and fully quantized low-bit vision transformer. In *Advances in Neural Information Processing Systems*, pages 34451–34463, 2022. 1, 2
- [45] Zhikai Li and Qingyi Gu. I-ViT: Integer-only quantization for efficient vision transformer inference. In *Proceedings of the IEEE/CVF International Conference on Computer Vision*, pages 17065–17075, 2023. 5, 6
- [46] Ji Lin, Jiaming Tang, Haotian Tang, Shang Yang, Wei-Ming Chen, Wei-Chen Wang, Guangxuan Xiao, Xingyu Dang, Chuang Gan, and Song Han. AWQ: Activation-aware weight quantization for on-device llm compression and acceleration. In *Proceedings of Machine Learning and Systems*, pages 87–100, 2024. 1, 2
- [47] Tsung-Yi Lin, Michael Maire, Serge Belongie, James Hays, Pietro Perona, Deva Ramanan, Piotr Dollár, and C Lawrence Zitnick. Microsoft COCO: Common objects in context. In *European Conference on Computer Vision*, pages 740–755. Springer, 2014. 7
- [48] Haotian Liu, Chunyuan Li, Qingyang Wu, and Yong Jae Lee. Visual instruction tuning. In *Advances in Neural Information Processing Systems*, pages 34892–34916, 2023. 1
- [49] Ze Liu, Yutong Lin, Yue Cao, Han Hu, Yixuan Wei, Zheng Zhang, Stephen Lin, and Baining Guo. Swin Transformer: Hierarchical vision transformer using shifted windows. In *Proceedings of the IEEE/CVF International Conference on Computer Vision*, pages 10012–10022, 2021. 1, 9
- [50] Zhenhua Liu, Yunhe Wang, Kai Han, Wei Zhang, Siwei Ma, and Wen Gao. Post-training quantization for vision transformer. In *Advances in Neural Information Processing Systems*, pages 28092–28103, 2021. 1, 2
- [51] Zechun Liu, Barlas Oguz, Changsheng Zhao, Ernie Chang, Pierre Stock, Yashar Mehdad, Yangyang Shi, Raghuraman

- Krishnamoorthi, and Vikas Chandra. LLM-QAT: Data-free quantization aware training for large language models. *arXiv preprint arXiv:2305.17888*, 2023. 1, 2
- [52] Nanye Ma, Mark Goldstein, Michael S Albergo, Nicholas M Boffi, Eric Vanden-Eijnden, and Saining Xie. SiT: Exploring flow and diffusion-based generative models with scalable interpolant transformers. In *European Conference on Computer Vision*, pages 23–40. Springer, 2024. 8
- [53] Charlie Nash, Jacob Menick, Sander Dieleman, and Peter W Battaglia. Generating images with sparse representations. *arXiv preprint arXiv:2103.03841*, 2021. 8
- [54] Eric Nguyen, Karan Goel, Albert Gu, Gordon Downs, Preey Shah, Tri Dao, Stephen Baccus, and Christopher Ré. S4ND: Modeling images and videos as multidimensional signals with state spaces. In *Advances in Neural Information Processing Systems*, pages 2846–2861, 2022. 2, 5, 6
- [55] Adam Paszke, Sam Gross, Francisco Massa, Adam Lerer, James Bradbury, Gregory Chanan, Trevor Killeen, Zeming Lin, Natalia Gimelshein, Luca Antiga, et al. Pytorch: An imperative style, high-performance deep learning library. In *Advances in Neural Information Processing Systems*, 2019. 5
- [56] William Peebles and Saining Xie. Scalable diffusion models with transformers. In *Proceedings of the IEEE/CVF International Conference on Computer Vision*, pages 4195–4205, 2023. 1, 8
- [57] Hadi Pouransari, Zhucheng Tu, and Oncel Tuzel. Least squares binary quantization of neural networks. In *Proceedings of the IEEE/CVF Conference on Computer Vision and Pattern Recognition Workshops*, pages 698–699, 2020. 3
- [58] Panjie Qi, Edwin Hsing-Mean Sha, Qingfeng Zhuge, Hongwu Peng, Shaoyi Huang, Zhenglun Kong, Yuhong Song, and Bingbing Li. Accelerating framework of transformer by hardware design and model compression co-optimization. In *2021 IEEE/ACM International Conference On Computer Aided Design (ICCAD)*, pages 1–9. IEEE, 2021. 1
- [59] Alec Radford, Jong Wook Kim, Chris Hallacy, Aditya Ramesh, Gabriel Goh, Sandhini Agarwal, Girish Sastry, Amanda Askell, Pamela Mishkin, Jack Clark, et al. Learning transferable visual models from natural language supervision. In *International Conference on Machine Learning*, pages 8748–8763. PMLR, 2021. 1
- [60] Colin Raffel, Noam Shazeer, Adam Roberts, Katherine Lee, Sharan Narang, Michael Matena, Yanqi Zhou, Wei Li, and Peter J Liu. Exploring the limits of transfer learning with a unified text-to-text transformer. *Journal of Machine Learning Research*, 21(140):1–67, 2020. 1
- [61] Mohammad Rastegari, Vicente Ordonez, Joseph Redmon, and Ali Farhadi. XNOR-Net: ImageNet classification using binary convolutional neural networks. In *European Conference on Computer Vision*, pages 525–542. Springer, 2016. 6
- [62] Nikhila Ravi, Valentin Gabeur, Yuan-Ting Hu, Ronghang Hu, Chaitanya Ryali, Tengyu Ma, Haitham Khedr, Roman Rädle, Chloe Rolland, Laura Gustafson, et al. SAM 2: Segment anything in images and videos. *arXiv preprint arXiv:2408.00714*, 2024. 1
- [63] Aurko Roy, Mohammad Saffar, Ashish Vaswani, and David Grangier. Efficient content-based sparse attention with routing transformers. *Transactions of the Association for Computational Linguistics*, 9:53–68, 2021. 1, 2
- [64] Tim Salimans, Ian Goodfellow, Wojciech Zaremba, Vicki Cheung, Alec Radford, and Xi Chen. Improved techniques for training gans. In *Advances in Neural Information Processing Systems*, 2016. 8
- [65] Jay Shah, Ganesh Bikshandi, Ying Zhang, Vijay Thakkar, Pradeep Ramani, and Tri Dao. FlashAttention-3: Fast and accurate attention with asynchrony and low-precision. In *Advances in Neural Information Processing Systems*, pages 68658–68685, 2024. 2, 3
- [66] Zhuoran Shen, Mingyuan Zhang, Haiyu Zhao, Shuai Yi, and Hongsheng Li. Efficient Attention: Attention with linear complexities. In *Proceedings of the IEEE/CVF Winter Conference on Applications of Computer Vision*, pages 3531–3539, 2021. 5, 6
- [67] Yehui Tang, Yunhe Wang, Jianyuan Guo, Zhijun Tu, Kai Han, Hailin Hu, and Dacheng Tao. A survey on transformer compression. *arXiv preprint arXiv:2402.05964*, 2024. 1
- [68] Jiale Tao, Yanbing Zhang, Qixun Wang, Yiji Cheng, Haofan Wang, Xu Bai, Zhengguang Zhou, Ruihuang Li, Linqing Wang, Chunyu Wang, et al. Instantcharacter: Personalize any characters with a scalable diffusion transformer framework. *arXiv preprint arXiv:2504.12395*, 2025. 1
- [69] Yi Tay, Dara Bahri, Liu Yang, Donald Metzler, and Da-Cheng Juan. Sparse sinkhorn attention. In *International Conference on Machine Learning*, pages 9438–9447. PMLR, 2020. 1, 2
- [70] Yi Tay, Mostafa Dehghani, Dara Bahri, and Donald Metzler. Efficient Transformers: A survey. *ACM Computing Surveys*, 55(6), 2022. 1
- [71] Gemini Team, Petko Georgiev, Ving Ian Lei, Ryan Burnell, Libin Bai, Anmol Gulati, Garrett Tanzer, Damien Vincent, Zhufeng Pan, Shibo Wang, et al. Gemini 1.5: Unlocking multimodal understanding across millions of tokens of context. *arXiv preprint arXiv:2403.05530*, 2024. 1
- [72] Hugo Touvron, Matthieu Cord, Matthijs Douze, Francisco Massa, Alexandre Sablayrolles, and Hervé Jégou. Training data-efficient image transformers & distillation through attention. In *International Conference on Machine Learning*, pages 10347–10357. PMLR, 2021. 6, 8, 15
- [73] Hugo Touvron, Thibaut Lavril, Gautier Izacard, Xavier Martinet, Marie-Anne Lachaux, Timothée Lacroix, Baptiste Rozière, Naman Goyal, Eric Hambro, Faisal Azhar, et al. LLaMA: Open and efficient foundation language models. *arXiv preprint arXiv:2302.13971*, 2023. 1
- [74] Ashish Vaswani, Noam Shazeer, Niki Parmar, Jakob Uszkoreit, Llion Jones, Aidan N Gomez, Łukasz Kaiser, and Illia Polosukhin. Attention is all you need. In *Advances in Neural Information Processing Systems*, 2017. 1, 3
- [75] Peng Wang, Shuai Bai, Sinan Tan, Shijie Wang, Zhihao Fan, Jinze Bai, Keqin Chen, Xuejing Liu, Jialin Wang, Wenbin Ge, et al. Qwen2-VL: Enhancing vision-language model’s perception of the world at any resolution. *arXiv preprint arXiv:2409.12191*, 2024. 1
- [76] Sinong Wang, Belinda Z Li, Madian Khabsa, Han Fang, and Hao Ma. Linformer: Self-attention with linear complexity. *arXiv preprint arXiv:2006.04768*, 2020. 1, 2

- [77] Yuxin Wu, Alexander Kirillov, Francisco Massa, Wan-Yen Lo, and Ross Girshick. Detectron2. <https://github.com/facebookresearch/detectron2>, 2019. 7
- [78] Guangxuan Xiao, Yuandong Tian, Beidi Chen, Song Han, and Mike Lewis. Efficient streaming language models with attention sinks. *arXiv preprint arXiv:2309.17453*, 2023. 1, 2
- [79] Junrui Xiao, Zhikai Li, Jianquan Li, Lianwei Yang, and Qingyi Gu. BinaryViT: Towards efficient and accurate binary vision transformers. *IEEE Transactions on Circuits and Systems for Video Technology*, 2024. 1, 2
- [80] Tete Xiao, Yingcheng Liu, Bolei Zhou, Yuning Jiang, and Jian Sun. Unified perceptual parsing for scene understanding. In *European Conference on Computer Vision*, pages 418–434, 2018. 7
- [81] Jiwei Yang, Xu Shen, Jun Xing, Xinmei Tian, Houqiang Li, Bing Deng, Jianqiang Huang, and Xian-sheng Hua. Quantization networks. In *Proceedings of the IEEE/CVF Conference on Computer Vision and Pattern Recognition*, pages 7308–7316, 2019. 1, 2
- [82] Songlin Yang, Bailin Wang, Yu Zhang, Yikang Shen, and Yoon Kim. Parallelizing linear transformers with the delta rule over sequence length. In *Advances in Neural Information Processing Systems*, pages 115491–115522, 2024. 1, 2
- [83] Haoran You, Yunyang Xiong, Xiaoliang Dai, Bichen Wu, Peizhao Zhang, Haoqi Fan, Peter Vajda, and Yingyan Lin. Castling-Vit: Compressing self-attention via switching towards linear-angular attention during vision transformer inference. *arXiv preprint arXiv:2211.10526*, 2022. 5, 6
- [84] Weihao Yu, Mi Luo, Pan Zhou, Chenyang Si, Yichen Zhou, Xinchao Wang, Jiashi Feng, and Shuicheng Yan. Metaformer is actually what you need for vision. In *Proceedings of the IEEE/CVF Conference on Computer Vision and Pattern Recognition*, pages 10819–10829, 2022. 1, 2
- [85] Jingyang Yuan, Huazuo Gao, Damai Dai, Junyu Luo, Liang Zhao, Zhengyan Zhang, Zhenda Xie, YX Wei, Lean Wang, Zhiping Xiao, et al. Native sparse attention: Hardware-aligned and natively trainable sparse attention. *arXiv preprint arXiv:2502.11089*, 2025. 1, 2
- [86] Zhihang Yuan, Chenhao Xue, Yiqi Chen, Qiang Wu, and Guangyu Sun. PTQ4ViT: Post-training quantization for vision transformers with twin uniform quantization. In *European Conference on Computer Vision*, pages 191–207. Springer, 2022. 5, 6
- [87] Jintao Zhang, Haofeng Huang, Pengle Zhang, Jia Wei, Jun Zhu, and Jianfei Chen. SageAttention2: Efficient attention with thorough outlier smoothing and per-thread int4 quantization. In *International Conference on Machine Learning*, 2025. 1, 2, 3
- [88] Jintao Zhang, Jia Wei, Pengle Zhang, Xiaoming Xu, Haofeng Huang, Haoxu Wang, Kai Jiang, Jun Zhu, and Jianfei Chen. SageAttention3: Microscaling FP4 attention for inference and an exploration of 8-bit training. In *The Thirty-ninth Annual Conference on Neural Information Processing Systems*, 2025. 2
- [89] Jintao Zhang, Jia Wei, Pengle Zhang, Jun Zhu, and Jianfei Chen. SageAttention: Accurate 8-bit attention for plug-and-play inference acceleration. In *International Conference on Learning Representations*, 2025. 1, 2, 3, 5, 6, 14
- [90] Bolei Zhou, Hang Zhao, Xavier Puig, Tete Xiao, Sanja Fidler, Adela Barriuso, and Antonio Torralba. Semantic understanding of scenes through the ADE20K dataset. *International Journal of Computer Vision*, 127(3):302–321, 2019. 7
- [91] Lianghui Zhu, Bencheng Liao, Qian Zhang, Xinlong Wang, Wenyu Liu, and Xinggang Wang. Vision Mamba: Efficient visual representation learning with bidirectional state space model. In *International Conference on Machine Learning*, 2024. 2, 5, 6

BinaryAttention: One-Bit QK-Attention for Vision and Diffusion Transformers

Supplementary Material

In this supplementary file, we provide following materials:

- A Proof of Theorem 1 (referring to Sec. 4.1 in the main paper);
- B Algorithm of BinaryAttention (referring to Sec. 4.3 in the main paper);
- C Experimental details in classification (referring to Sec. 5.1 in the main paper);
- D More qualitative comparisons (referring to Sec. 5.5 in the main paper).

A. Proof of Theorem 1

Proof. Consider the element (i, j) of the matrix st^T :

$$[st^T]_{ij} = s_i t_j = \text{sign}(\mathbf{q}_i) \text{sign}(\mathbf{k}_j).$$

Since \mathbf{q} and \mathbf{k} are assumed to be jointly Gaussian with zero-mean, the pair $(\mathbf{q}_i, \mathbf{k}_j)$ is also jointly Gaussian. We have:

$$\begin{aligned} \text{Var}(\mathbf{q}_i) &= \Sigma_{qq}[i, i], \quad \text{Var}(\mathbf{k}_j) = \Sigma_{kk}[j, j], \\ \text{Cov}(\mathbf{q}_i, \mathbf{k}_j) &= \Sigma_{qk}[i, j]. \end{aligned}$$

Then the correlation of \mathbf{q}_i and \mathbf{k}_j is given by:

$$\rho_{ij} = \frac{\Sigma_{qk}[i, j]}{\sqrt{\Sigma_{qq}[i, i] \Sigma_{kk}[j, j]}} = C_{ij}.$$

Let $x = \Sigma_{qq}^{-\frac{1}{2}}[i, i] \mathbf{q}_i$ and $y = \Sigma_{kk}^{-\frac{1}{2}}[j, j] \mathbf{k}_j$, then the two variables x, y are standard Gaussian with correlation ρ_{ij} , and the joint density can be expressed as:

$$p(x, y) = \frac{1}{2\pi\sqrt{1-\rho_{ij}^2}} \exp\left(-\frac{x^2 - 2\rho_{ij}xy + y^2}{2(1-\rho_{ij}^2)}\right).$$

We now calculate the expectation of $\text{sign}(x)\text{sign}(y)$, where

$$\text{sign}(x)\text{sign}(y) = \begin{cases} +1 & \text{if } x \geq 0, y \geq 0 \text{ or } x \leq 0, y \leq 0 \\ -1 & \text{if } x \geq 0, y < 0 \text{ or } x < 0, y \geq 0 \end{cases}.$$

By the symmetry of standard Gaussian, we have

$$\mathbb{E}[\text{sign}(x)\text{sign}(y)] = 4\mathbb{P}(x \geq 0, y \geq 0) - 1.$$

Since

$$\begin{aligned} \mathbb{P}(x \geq 0, y \geq 0) &= \int_0^\infty \int_0^\infty p(x, y) dx dy \stackrel{\substack{x=R \cos \theta \\ y=R \sin \theta}}{\longrightarrow} \\ &= \frac{1}{2\pi\sqrt{1-\rho_{ij}^2}} \int_0^{\frac{\pi}{2}} \int_0^\infty \exp\left(-\frac{R^2(1-\rho_{ij} \sin 2\theta)}{2(1-\rho_{ij}^2)}\right) R dR d\theta \\ &= \frac{1}{2\pi} \arcsin \rho_{ij} + \frac{1}{4}, \end{aligned}$$

we have:

$$\mathbb{E}[\text{sign}(x)\text{sign}(y)] = \frac{2}{\pi} \arcsin \rho_{ij} = \frac{2}{\pi} \arcsin C_{ij}.$$

Note that the $\text{sign}(\cdot)$ function is scale-invariant for any strictly positive scales, we can ensure that

$$\mathbb{E}[\text{sign}(\mathbf{q}_i)\text{sign}(\mathbf{k}_j)] = \mathbb{E}[\text{sign}(x)\text{sign}(y)] = \frac{2}{\pi} \arcsin C_{ij}.$$

Since it holds for all $i, j = 1, \dots, d$, there is:

$$\mathbb{E}[st^T] = \frac{2}{\pi} \arcsin C.$$

□

B. Algorithm of BinaryAttention

Our implementation of BinaryAttention is built upon the fundamental principles of FlashAttention2 [13] and SageAttention [89] while introducing specialized optimizations for binary and low-precision computations. The complete algorithm is presented in Algorithm 1.

Algorithm 1: Implementation of BinaryAttention

Input: Matrices $\mathbf{Q}, \mathbf{K}, \mathbf{V} \in \mathbb{R}^{N \times d}$, bias $\mathbf{B} \in \mathbb{R}^{N \times N}$, block size B_r, B_v .

Output: Matrices $\mathbf{O} \in \mathbb{R}^{N \times d}$.

1 Processing:

$(\mu_q, \mathbf{S}) \leftarrow \phi(\mathbf{Q}), (\mu_k, \mathbf{T}) \leftarrow \phi(\mathbf{K}), (\delta_v, \tilde{\mathbf{V}}) \leftarrow \psi(\mathbf{V});$
// Quantization by Eq. (5) and Eq. (7)

2 Divide \mathbf{S}, \mathbf{O} into $T_r := \lceil N/B_r \rceil$ blocks $\{\mathbf{S}_i\}$ and $\{\mathbf{O}_i\}$;

3 Divide $\mathbf{T}, \tilde{\mathbf{V}}$ into $T_v := \lceil N/B_v \rceil$ blocks $\{\mathbf{T}_j\}$ and $\{\tilde{\mathbf{V}}_j\}$;

4 Divide \mathbf{B} into $T_r \times T_v$ blocks $\{\mathbf{B}_{ij}\}$; *// if bias*

5 for $i = 1$ **to** T_r **do**

6 Load block \mathbf{S}_i from HBM to SRAM;

7 Initialize

$\mathbf{O}_{i,0} = (0)_{B_r \times d}, l_{i,0} = (0)_{B_r}, m_{i,0} = (-\infty)_{B_r}$;

8 for $j = 1$ **to** T_v **do**

9 Load blocks $\mathbf{T}_j, \tilde{\mathbf{V}}_j, \mathbf{B}_{ij}$ from HBM to SRAM;

10 $\mathbf{S}_{ij} \leftarrow \text{BinaryMatmul}(\mathbf{S}_i, \mathbf{T}_j) \times \mu_q \times \mu_k$;

11 $\mathbf{S}_{ij} \leftarrow \mathbf{S}_{ij} + \mathbf{B}_{ij}$; *// if bias*

12 $m_{ij} \leftarrow \max(m_{i,j-1}, \text{rowmax}(\mathbf{S}_{ij}))$;

13 $\hat{\mathbf{P}}_{ij} \leftarrow \exp(\mathbf{S}_{ij} - m_{ij})$;

14 $l_{ij} \leftarrow e^{m_{i,j-1} - m_{ij}} l_{i,j-1} + \text{rowsum}(\hat{\mathbf{P}}_{ij})$;

15 $\mathbf{O}_{ij} \leftarrow \text{IntMatmul}(\hat{\mathbf{P}}_{ij} \times 255, \tilde{\mathbf{V}}_j)$;

16 $\mathbf{O}_{ij} \leftarrow \text{diag}(e^{m_{i,j-1} - m_{ij}})^{-1} \mathbf{O}_{ij} + \mathbf{O}_{ij}$;

17 end

18 $\mathbf{O}_i \leftarrow \text{diag}(l_{i,T_v})^{-1} \mathbf{O}_{i,T_v} / 255 \times \delta_v$;

19 Write \mathbf{O}_i ;

20 end

21 return $\mathbf{O} = \{\mathbf{O}_i\}$.

C. Experimental Details in Classification

Settings. We benchmark BinaryAttention on ImageNet-1K [16] dataset. Following the experimental configurations of DeiT [72], we employ the AdamW optimizer for 300 epochs with beta set to (0.9, 0.999), momentum of 0.9 and a batch size of 1024. An initial learning rate of 10^{-4} , a minimum learning rate of 10^{-5} and a weight decay of 0.02 are used. The learning rate follows a cosine annealing schedule with a warm-up of 5 epochs. We include commonly used augmentation and regularization strategies, consistent with the training of DeiT. The drop path rate is set to 0.1 for all BinaryAttention variants. Before training, the models are initialized with full-precision pre-trained weights. We utilize the self-distillation strategy with the full-precision counterpart as teacher, and implement quantization-aware training with Straight-Through Estimators (STE) [4]. For the input resolution of 384×384 , we continue to fine-tune the models for 30 epochs, with a batch size of 512, a constant learning rate of 10^{-5} , and a weight decay of 10^{-8} .

Epochs	DeiT-T	DeiT-S	DeiT-B
Baseline	72.2	79.8	81.8
100	71.98	79.44	81.80
300	72.44	79.97	81.99

Table 9. Top-1 accuracy of DeiT models using BinaryAttention without bias at 100 and 300 fine-tuning epochs.

Tuning Cost. In extreme low-bit quantization, fine-tuning is a standard and necessary step to bridge performance gaps. While training-free methods prioritize convenience, their performance is strictly limited by the baseline, whereas BinaryAttention raises the accuracy. For the best performance,

we employ a fine-tuning schedule of 300 epochs, which is consistent with common practice in low-bit approaches such as BiViT [31]. We further report the performance at different fine-tuning epochs in Tab. 9. It can be seen that with 100 fine-tuning epochs, BinaryAttention already nearly matches the baseline, with Top-1 accuracy gaps of 0.22/0.36/0.00 on DeiT-T/S/B, respectively. Extending fine-tuning to 300 epochs not only recovers the baseline performance but yields a modest improvement.

D. More Qualitative Comparisons

Fig. 6 provides more qualitative comparisons of FlashAttention2, SageAttention, and BinaryAttention, showing additional images generated by the DiT-XL/2 model (cfg=1.50). We can see that SageAttention and FlashAttention2 produce nearly identical images, while BinaryAttention produces slightly different content but maintains competitive generation quality with sufficient details.



Figure 6. More qualitative comparisons of generated image by DiT-XL/2 (cfg=1.50) using FlashAttention2, SageAttention and BinaryAttention.